ORGANIC CHEMISTRY FRONTIERS

RESEARCH ARTICLE

View Article Online
View Journal | View Issue

Check for updates

Cite this: *Org. Chem. Front.*, 2022, **9**, 4250

Bis-borylated arylisoquinoline-derived dyes with a central aromatic core: towards efficient fluorescent singlet-oxygen photosensitizers†‡

René Campos-González, §[a,b] Pablo Vázquez-Domínguez,§[c,d] Patricia Remón,[a] Francisco Nájera, [e,f] Daniel Collado,[e,f] Ezequiel Pérez-Inestrosa, [e,f] Francisco Boscá,[g] Abel Ros *[c] and Uwe Pischel *[a]

Received 13th May 2022,
Accepted 19th June 2022

DOI: 10.1039/d2qo00778a

rsc.li/frontiers-organic

Conveniently modified polycyclic aromatic hydrocarbon (PAH) fluorophores are obtained by a bromination–borylation sequence. The bis-borylated dyes show red-shifted absorption ($\lambda_{abs,max}$ > 450 nm) and emission ($\lambda_{f,max}$ > 500 nm; Φ_f: 0.3–0.5) properties as compared to the parent PAHs. Their centrosymmetric A–π-A (A: acceptor) structures led to the observation of two-photon absorption (up to 60 GM) in the near-infrared spectral region (>800 nm). The rigid structure shuts down non-radiative deactivation by limiting rotational or vibrational freedom. Thus, the excited-state pathways originating from the excited singlet state are resumed to fluorescence and excited triplet-state formation. The latter is involved in the energy-transfer sensitization of singlet oxygen (Φ_Δ: 0.50–0.66). This bipartition provides the setting for the concomitant observation of fluorescence and photosensitization, making these dyes ideal bimodal chromophores.

Open Access Article. Published on 29 2022. Downloaded on 12/13/2025 6:14:51 PM.
This article is licensed under a Creative Commons Attribution-NonCommercial 3.0 Unported Licence.

Introduction

Robust emissive dyes, whose fluorescence properties can be fine-tuned by the modification of their electronic structure, are prime candidates for optoelectronic applications and functional materials. Special focus has been placed on organoboron fluorophores, where the boron centre is encountered in either a three- or four-coordinate state.[1–6] In the former state, the electron-deficient boron, featuring an empty $2p_\pi$ orbital, may play the role of an electron acceptor. When integrated with electron donors, highly interesting architectures, which serve as photoinduced electron-transfer and charge-transfer model systems[3,6–9] or two-photon-absorbing fluorophores,[10–15] have been obtained.

Four-coordinate boron provides a stable octet valence situation, deriving from the interaction of the three-coordinate element with an additional Lewis base.[1,4,5,16–27] In this context, the integration of classical polycyclic aromatic hydrocarbons (PAHs) with N,C chelate organoboron structural moieties has enjoyed notable preference.[21,28–33] In these dyes, the BN Lewis pair introduces structural and electronic variations that have direct consequences for the photophysical properties, resulting in red-shifted optical spectra and improved emission quantum yields when compared to the corresponding PAH core alone. In Fig. 1, representative examples for such dyes are shown. A bis-borylated dye with the smallest aromatic PAH core, *i.e.*, benzene, was reported by the Nowak-Król group.[34] Structure **A** is prepared by a modular synthetic approach and shows helical chirality. The Wang group introduced structure **B**, showing interesting photochemical reactivity,[35] similar to earlier systems that were based on (ppy)$BMes_2$ (ppy = 2-phenylpyridine).[28] Substituting the pyridyl unit with an isoquinolyl enabled our group to design arylisoquinoline-derived fluorophores with naphthyl (structures **C** with varying electron-donating substituents R) or anthryl (structure **D**).[21] Structures **C** were shown to feature intramolecular charge-transfer fluorescence, implying significant solvatofluorochro-

[a]*CIQSO – Centre for Research in Sustainable Chemistry and Department of Chemistry, University of Huelva, Campus de El Carmen s/n, 21071 Huelva, Spain. E-mail: uwe.pischel@diq.uhu.es*
[b]*Facultad de Química, Departamento de Química Orgánica, Universidad Nacional Autónoma de México, Cto. Exterior s/n, Coyoacán, 04510 Ciudad de México, Mexico*
[c]*Institute for Chemical Research, CSIC-US, C/Américo Vespucio 49, 41092 Seville, Spain. E-mail: abel.ros@iiq.csic.es*
[d]*Department of Organic Chemistry, Innovation Centre in Advanced Chemistry, ORFEO-CINQA, University of Seville, C/Prof. García González 1, 41012 Seville, Spain*
[e]*Department of Organic Chemistry, IBIMA, University of Málaga, Campus Teatinos s/n, 29071 Málaga, Spain*
[f]*Andalusian Centre for Nanomedicine and Biotechnology, BIONAND, Parque Tecnológico de Andalucía, 29590 Málaga, Spain*
[g]*Instituto de Tecnología Química, Universitat Politècnica de València – Consejo Superior de Investigaciones Científicas, Avda. de los Naranjos s/n, 46022 Valencia, Spain*

† Dedicated to the memory of Professor John S. Fossey.

‡ Electronic supplementary information (ESI) available. See DOI: https://doi.org/10.1039/d2qo00778a

§ These authors contributed equally.

This journal is © the Partner Organisations 2022

Open Access Article. Published on 29 2022. Downloaded on 12/13/2025 6:14:51 PM.
This article is licensed under a Creative Commons Attribution-NonCommercial 3.0 Unported Licence.

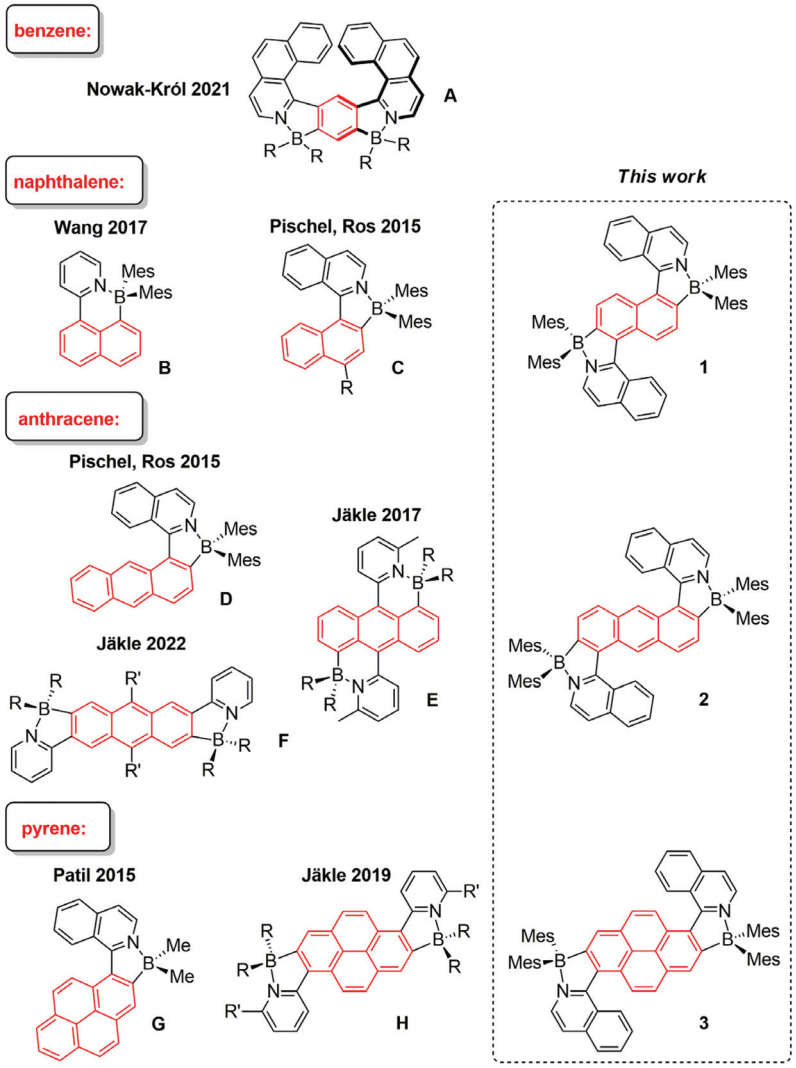

Fig. 1 Representative examples of PAHs that are structurally integrated with BN Lewis pairs and structures of the herein investigated dyes **1–3**. Please note that formal charges at B (negative) and N (positive) are not shown, as commonly practiced in the field.

mism and large Stokes shifts. The Jäkle group has used BN Lewis-pair formation to extend the anthracene skeleton laterally (structure **E**)[32] or linearly (structure **F**).[36] This yielded red-shifted fluorescence, as compared to simple anthracene dyes, and photosensitized singlet-oxygen ($^1O_2$) formation. Using pyrene as the aromatic core led for example to structures **G** and **H**.[31,33]

Chromophores that exhibit efficient fluorescence, but also populate enough excited triplet state that could trigger the formation of $^1O_2$, are of interest because of their bimodal activity. Such dyes/photosensitizers could be spatially located through their fluorescence and would at the same time lead to the generation of therapeutically active $^1O_2$, as for example, implied in photodynamic therapy (PDT) of tumorous tissues.[37–39] In the context of organoboron structures, $^1O_2$-photosensitizing BODIPY dyes often include heavy atoms (bromine, iodine) to promote the population of the excited triplet state, which in turn is implied in energy transfer to triplet oxygen.[38,40] Accordingly, high $^1O_2$ formation quantum yields (Φ_Δ) are observed for these dyes (typically 0.8–0.9), but relatively low fluorescence quantum yields (Φ_f), typically smaller than 0.1, result. As the implicated excited singlet and triplet manifolds are antagonists, communicated by intersystem crossing (ISC), any exaggeration of fluorescence or $^1O_2$ formation would have detrimental effects on the opposed mechanism. Hence, when striving for dyes that act simultaneously as good fluorophores and photosensitizers, it is desirable that the implied excited-state mechanisms are in balance (Scheme 1), *i.e.*, $\Phi_\Delta \sim \Phi_f \sim 0.5$. This would require that (i) non-radiative excited singlet-state deactivation pathways, other than the population of triplet state by ISC, are disfavored and that (ii) the energy transfer (ET) between the excited triplet state of the dye and triplet oxygen proceeds quantitatively.

Herein we synthesized three bis-borylated PAHs (structures **1–3** in Fig. 1), which enlarge the pool of related tetracoordinate organoboron dyes structurally and functionally. For example,

Open Access Article. Published on 29 2022. Downloaded on 12/13/2025 6:14:51 PM.
This article is licensed under a Creative Commons Attribution-NonCommercial 3.0 Unported Licence.

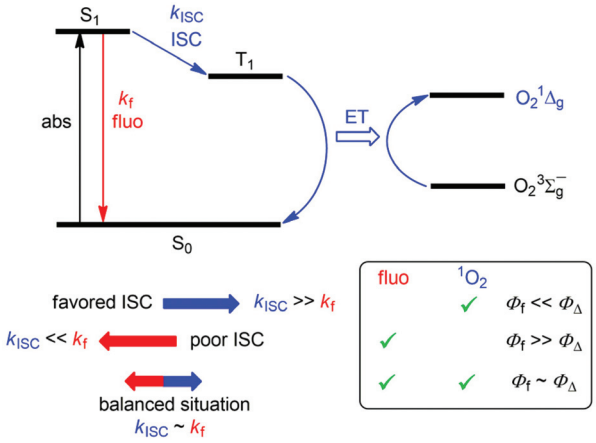

Scheme 1 Jablonski diagram for the correlation between fluorescence and $^1O_2$ formation. ISC: intersystem crossing, ET: energy transfer.

the anthracene-derived dye **2**, which could be termed as a "diagonally extended" structure, fills the structural gap between **E** and **F**, recently published by the Jäkle group.[32] The highlights of the photophysical performance of the new dyes are remarkable $^1O_2$ photosensitization and maintenance of significant fluorescence. The formation of $^1O_2$ was directly evidenced and quantified by observing its near-infrared (NIR) phosphorescence emission. The sensitization quality was related to the characteristics of the excited triplet state precursors, as obtained from time-resolved transient absorption spectroscopy, yielding a detailed photomechanistic picture. In addition, the new dyes were found to be active in two-photon absorption, which adds a further dimension to their photofunctional behavior. This provides the possibility to excite the dyes with low-energy NIR light, reaching the same excited states as observed for conventional one-photon excitation.

Results and discussion

Synthesis

The synthesis of the dyes **1–3** is summarized in Scheme 2. Starting from the diboronic pinacolate esters **1A–3A**,[41,42] the $Pd(PPh_3)_4$-catalyzed Suzuki coupling with 1-chloroisoquinoline afforded the triarylic systems **1B–3B** as a mixture of rotamers in 61–78% yield. These were then transformed into the corresponding *o*,*o*′-dibrominated products **1C–3C** by employing our previously described C–H borylation/bromination methodology.[21,27,43] The nitrogen-directed C–H borylation was carried out by using excess B_2pin_2 (pin = pinacolate) and $[Ir(\mu\text{-}OMe)(cod)]_2$ (cod = 1,5-cyclooctadiene) as the catalyst in combination with 2-pyridinecarboxaldehyde *N*,*N*-dibenzylhydrazone as the additional ligand.[43] Elevated temperatures (90–100 °C) and prolonged time (2–3 days) were necessary to complete the reaction. The crude products were used directly for the bromination with $CuBr_2$[21,27] and the dibromides **1C–3C** were obtained in 37–79% yield as *meso*/racemic mixtures. The isomers were separated by column chromatography and the

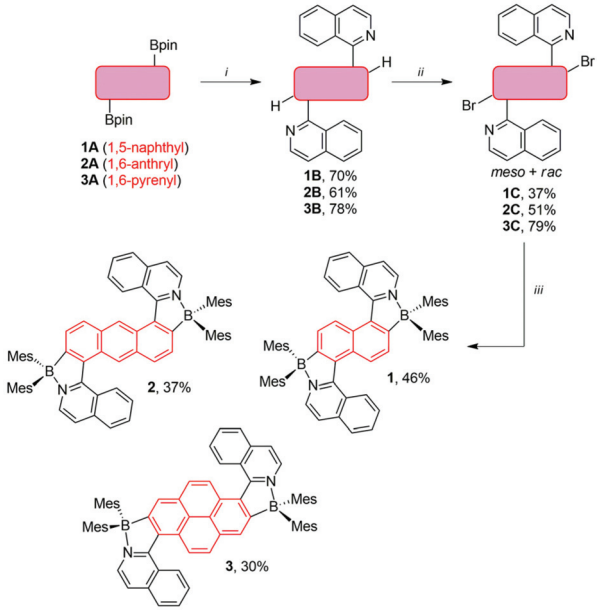

Scheme 2 Synthesis of the dyes **1–3**. (i) 2.6 equiv. 1-chloroisoquinoline, 6 mol% $[Pd(PPh_3)_4]$, toluene : MeOH (2 : 1), Na_2CO_3 (aq.), 90 °C. (ii)(1) 2.8 equiv. B_2pin_2, 4 mol% $[Ir(\mu\text{-}OMe)(cod)]_2$, 8 mol% 2-pyridinecarboxaldehyde *N*,*N*-dibenzylhydrazone, 1,4-dioxane, 90–100 °C. (2) 6.0 equiv. $CuBr_2$, i-PrOH : MeOH (2 : 3), water, 90 °C. (iii) (1) 2.4 equiv. *n*-BuLi, anhydrous THF, −78 °C. (2) 3.0 equiv. Mes_2BF (Mes: mesityl), −78 °C → rt.

one with the lower R_f was used further. However, due to their symmetric structure they could not be assigned based on their NMR spectra (see the ESI‡). Finally, the dibromides **1C–3C** were transformed into the diboranes **1–3** in a one-pot procedure consisting of a Br/Li exchange, followed by the reaction with Mes_2BF.[21,27] This afforded the dyes in 30–46% yield as yellow-orange amorphous solids.

The details of the analytical characterization (^1H, ^{13}C, ^{11}B NMR, and electrospray ionization mass spectrometry) can be found in the ESI.‡ Broad signals for methyl and aryl protons and carbons of mesityl groups were observed in the NMR spectra recorded at 25 °C. This is due to two factors. (i) There is significant degree of fluxionality, leading to configurational instability of the chiral axes. This is reasoned with the BN coordination, which opens up the angles around the chiral axes.[21] (ii) The rotation of the mesityl group around the B–CMes bond is very slow. Indeed, in the case of **2** and **3**, high-temperature NMR experiments (70 °C) were required to obtain well-defined spectra. The sp^3 character of the boron center was unambiguously confirmed by ^{11}B NMR spectroscopy, which revealed a resonance signal at 6.0–6.2 ppm for all dyes.[20,21]

One-photon optical spectroscopy

The dyes **1–3** were photophysically characterized by UV/vis absorption and fluorescence spectroscopy as well as by time-correlated single-photon-counting measurements (TCSPC), using toluene and tetrahydrofuran (THF) as solvents. The data

 This journal is © the Partner Organisations 2022

Open Access Article. Published on 29 2022. Downloaded on 12/13/2025 6:14:51 PM.
This article is licensed under a Creative Commons Attribution-NonCommercial 3.0 Unported Licence.

Table 1 Photophysical properties of the dyes **1–3** in air-equilibrated toluene and tetrahydrofuran solution

	λ_{abs} (nm) [ε (M^{-1} cm^{-1})]	λ_f (nm)	Φ_f [a]	τ_f [b] (ns)	k_r (10^7 s^{-1})	k_{nr} (10^7 s^{-1})	λ_{2PA} (nm) [σ_2 (GM)][c]	$\lambda_{2PA,fluo}$ (nm)
Toluene								
1	447 [13 700] 424 [13 200] 403 [13 300]	485	0.33	4.52	7.3	14.8	810 [29]	492
2	491 [17 400] 461 [13 100]	512 540 (sh)	0.30	3.95	7.6	17.7	830 [44] 870 [59] 940 [20]	515
3	495 [39 500] 467 [38 800]	519 548 (sh)	0.50	3.15	15.9	15.8	840 [61] 950 [8]	520
Tetrahydrofuran								
1	445 [14 400] 423 [13 500] 394 [13 600]	481	0.34	4.52	7.5	14.6		
2	487 [16 400] 459 [13 000]	516 541 (sh)	0.27	4.11	6.6	17.7		
3	484 [47 900] 459 [45 900]	515 543 (sh)	0.53	3.70	14.3	12.7		

[a] Experimental error fluorescence quantum yield: *ca.* 10%. Fluorescence quantum yields measured for de-aerated toluene solutions of the dyes: 0.38 (**1**), 0.33 (**2**), and 0.53 (**3**). [b] Experimental error fluorescence lifetime: *ca.* 5%. [c] TPA data were determined only for toluene solutions. Experimental error TPA cross-section: *ca.* 15%.

are summarized in Table 1 and the spectra in toluene are shown in Fig. 2 (see the ESI‡ for the spectra in THF).

Several general observations can be made straightforward from the data and spectra. All dyes show typical vibronic fine-structure in their absorption spectra, similar to the observations made for the parent PAHs. The same can be clearly affirmed for the fluorescence spectra of **2** and **3**. The identity of the emission was confirmed by the superposing absorption and excitation spectra. The Stokes shifts of the dyes are small (*e.g.*, 2090 cm^{-1} for **1**, 850 cm^{-1} for **2**, and 930 cm^{-1} for **3** in toluene), excluding significant structural changes or solvent reorganization in the excited state.[21,27] Furthermore, the fluorescence properties vary only little between the two solvents used herein (*i.e.*, toluene and THF).

All dyes show emission of cyan-to-green color (maxima are situated between *ca.* 485 nm and 520 nm). Dye **1**, as the least extended π-system, absorbs and emits at somewhat shorter wavelengths, while dyes **2** and **3** show comparably red-shifted absorption and emission spectra. The fluorescence quantum yields of 0.3 (dyes **1** and **2**) to 0.5 (dye **3**) characterize the new fluorophores as efficient emitters. This is accompanied by fluorescence lifetimes in the range of 3.0–4.5 ns. The rate constants of the non-radiative excited-state decay are found to be very similar for all three dyes, while dye **3** has a significantly higher radiative rate constant as compared to dye **1** or **2** (see data in Table 1), in accordance with the increased fluorescence quantum yield of **3**.

Two-photon excitation

Dyes **1–3** are of centrosymmetric nature and feature an A–π-A (A = acceptor; defined by the isoquinolinium units) electronic structure. These two characteristics are desirable for the observation of nonlinear optical phenomena, such as two-photon absorption (2PA).[12,44–51] The efficiency of 2PA, measured as cross-section σ_2, can be determined by monitoring the two-photon-excited fluorescence of the chromophores.[52] This was done for the excitation wavelength region from 730 nm to 1040 nm. The obtained data and 2PA spectra in toluene are shown in Table 1 and Fig. 3, respectively.

Dye **1**, as the chromophore with the least extended central π system, shows its 2PA band at the shortest wavelength (810 nm) and with a relatively low TPA cross-section (*ca.* 30 GM). The other two dyes show their maxima shifted to longer wavelengths (870 nm for **2** and 840 nm for **3**), in agreement with the increased π-conjugation. The cross-section at the 2PA maximum is higher for **2** and **3** and reaches similar values (*ca.* 60 GM) as those observed previously for related donor-substituted mono-borylated dipolar dyes with structure **C** [Fig. 1; R = OCH_3, $N(CH_3)_2$].[21] The order of magnitude compares well with those of other low-molecular-weight tetracoordinate organoboron dyes with similar conjugation level, such as the BODIPY dye skeleton (*ca.* 50–100 GM)[53–55] or the BASHY dye family (*ca.* 150–200 GM),[56,57] although more efficient 2PA-active boron-containing chromophores are known.[58,59] The 2PA spectra (dividing the wavelengths by 2) do not compare with the long-wavelength band of the one-photon absorption spectra. This provides a hint that the two-photon excitation does not imply the lowest excited state S_1, but a higher-lying state, such as S_2 (see also DFT calculations below).

However, obeying Kasha's rule, the emissive S_1 state is rapidly populated by internal conversion and the chromophores show the same fluorescence emission (see Fig. 3) as observed for one-photon excitation. The observed emission is indeed generated by 2PA, as evident from the log–log plot of the emission intensity *versus* the laser excitation power, yielding the expected slope of **2** for all dyes (see Fig. 3).

Quantum-mechanical calculations

The conclusions drawn from the photophysical characterization of the processes involving excited singlet states were vali-

Open Access Article. Published on 29 2022. Downloaded on 12/13/2025 6:14:51 PM.
This article is licensed under a Creative Commons Attribution-NonCommercial 3.0 Unported Licence.

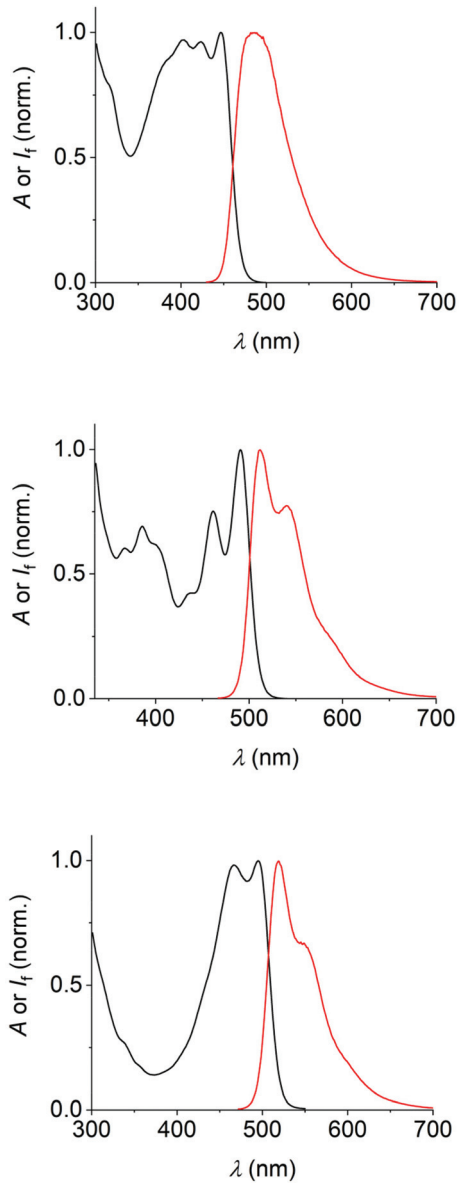

Fig. 2 UV/vis-absorption (black) and fluorescence spectra (red) of the dyes **1** (50 μM, top), **2** (25 μM, middle), and **3** (25 μM, bottom) in air-equilibrated toluene.

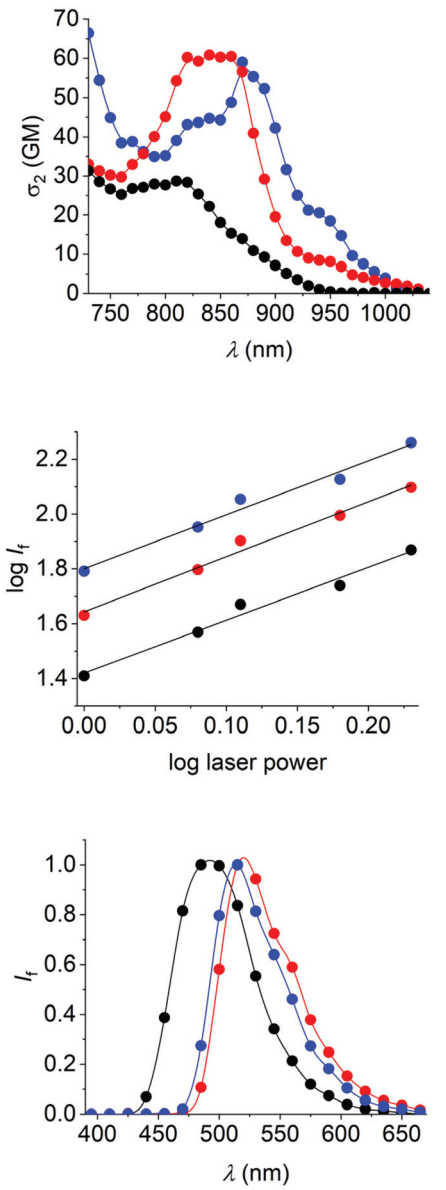

Fig. 3 Top: two-photon absorption spectra of **1**, **2**, and **3** in toluene. Middle: log–log plot of the two-photon excited fluorescence *versus* laser power. Bottom: two-photon excited fluorescence spectra. Colour code: **1**: black, **2**: blue, **3**: red.

dated by theoretical calculations at the PBE0/6-31G(d,p) level of theory.[60,61] The solvent (toluene) was taken into account by employing the polarization continuum model (PCM); see the ESI‡ for further details.[62]

In Table 2 the most significant information related to the absorption and emission of the dyes is summarized. The calculated absorption and emission energies are in very satisfactory agreement with the experimental values [difference of ≤0.07 eV; except for the emission energy of **3** (0.51 eV difference)].

The lowest energy $S_1 \leftarrow S_0$ (absorption) and $S_1 \rightarrow S_0$ (emission) transitions are dominated by the HOMO and LUMO frontier orbitals (FMOs). The HOMO/LUMO contour plots of the dyes **1**–**3** are shown in Fig. 4. For all three chromophores, it is easily visualized that the HOMO has its main incidence on the borylated central aromatic core and that the LUMO symmetrically involves both isoquinolinyl moieties. This affirms the assumed A–π-A quadrupolar electronic structure of the dyes and the observed 2PA activity.

The centrosymmetrical structures feature ^1A_g, ^1A_u, and ^1A_g symmetry for the S_0, S_1, and S_2 states, respectively. In accordance with the applicable selection rules, the $S_1 \leftarrow S_0$ transition is allowed in conventional one-photon absorption, while the $S_2 \leftarrow S_0$ transition cannot take place (zero oscillator strength). However, for the two-photon absorption, this is inversed and the $S_2 \leftarrow S_0$ transition is the active one.

This journal is © the Partner Organisations 2022

Open Access Article. Published on 29 2022. Downloaded on 12/13/2025 6:14:51 PM.
This article is licensed under a Creative Commons Attribution-NonCommercial 3.0 Unported Licence.

Table 2 DFT-calculated transition characteristics for the dyes **1–3**

	Absorption[a]		Emission[a]		2PA[b]	
	Transition [f][c] FMO contribution [%]	E_{max} (eV)	Transition [f][c] FMO contribution [%]	E_{max} (eV)	Transition	σ_2 (GM)
1	$S_1 \leftarrow S_0$ [0.311] LUMO ← HOMO [95]	2.81	$S_1 \rightarrow S_0$ [0.068] LUMO → HOMO [96]	2.29	$S_2 \leftarrow S_0$	41
2	$S_1 \leftarrow S_0$ [0.400] LUMO ← HOMO [98]	2.54	$S_1 \rightarrow S_0$ [0.427] LUMO → HOMO [98]	2.27	$S_2 \leftarrow S_0$	134
3	$S_1 \leftarrow S_0$ [0.701] LUMO ← HOMO [98]	2.44	$S_1 \rightarrow S_0$ [0.728] LUMO → HOMO [97]	2.16	$S_2 \leftarrow S_0$	57

[a] PBE0/6-31G(d,p) level of theory. [b] B3LYP/6-31G(d,p) level of theory. [c] Oscillator strength.

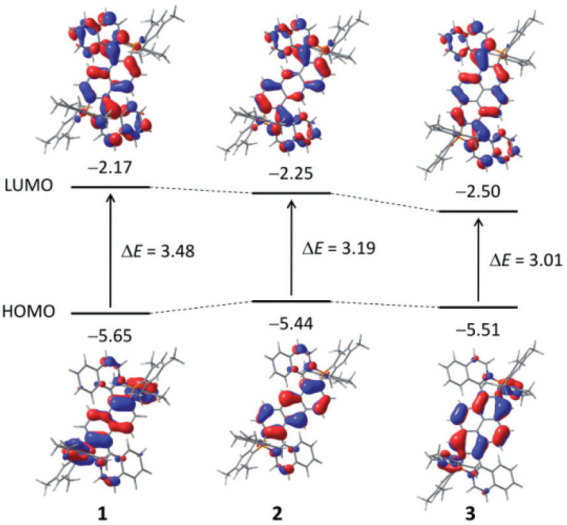

Fig. 4 HOMO–LUMO contour plots and energies for the dyes **1–3**.

Photosensitization of $^1O_2$ formation

Recently, related bis-borylated PAHs with anthracene as the central aromatic core (structures **E** and **F** in Fig. 1) have drawn attention as $^1O_2$ photosensitizers.[32,36] Transient absorption spectroscopy was performed on the herein investigated dyes to detect excited triplet states. These could serve as precursors for the formation of $^1O_2$ by means of energy transfer to triplet oxygen ($^3O_2$).

The transient spectra, obtained on nanosecond laser excitation of **1–3** in de-aerated toluene solution (see Fig. 5), show a negative signal. It coincides with the spectral position of the long-wavelength absorption of each dye (*i.e.*, 370–470 nm for dye **1**, 460–510 nm for dye **2**, and 410–520 nm for dye **3**) and also resembles the observed fine-structure. This signal is therefore ascribed to ground-state (GS) bleaching. The bleaching is overlapped with a transient spectrum of positive amplitude, featuring a broad band with a maximum at wavelengths longer

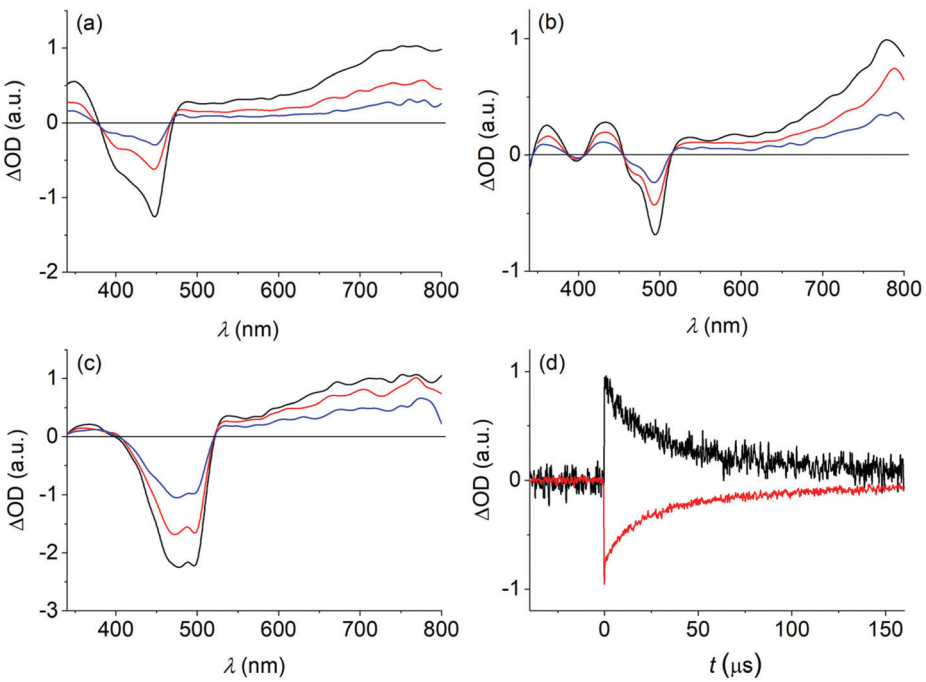

Fig. 5 Transient absorption spectra (λ_{exc} = 355 nm) of the dyes **1** (a), **2** (b), and **3** (c) at different time delays [1 (black), 20 (red), and 60 (blue) μs] in de-aerated toluene. In (d) the kinetic traces for dye **1** at λ_{obs} = 760 nm (black) and 450 nm (red) are shown.

Open Access Article. Published on 29 2022. Downloaded on 12/13/2025 6:14:51 PM.
This article is licensed under a Creative Commons Attribution-NonCommercial 3.0 Unported Licence.

Table 3 Transient spectroscopy data for dyes **1–3** in toluene

	1	2	3
GS bleaching			
λ_{max} (nm)	400 (sh)/450	470 (sh)/490	470 (sh)/500
τ (μs)	29	43	56
T–T absorption			
λ_{max} (nm)	760	780	760
k_q (O_2) (M^{-1} s^{-1})	1.0×10^9	9.5×10^8	1.0×10^9
τ (μs)	32	46	68
Φ_{ISC} [a]	0.63	0.56	0.51
$^1O_2$ formation			
Φ_Δ [b]	0.66	0.53	0.50

[a] Intersystem crossing (ISC) quantum yield; experimental error *ca.* 15%. [b] Quantum yield for $^1O_2$ formation; experimental error *ca.* 15%.

than 700 nm (*i.e.*, 760 nm for **1**, 780 nm for **2**, and 760 nm for **3**). The signal decays on the microsecond timescale (τ = 32–68 μs; see Table 3) and has practically the same kinetics as the recovery of the GS bleaching (see Fig. 5). Furthermore, the transient is quenched by oxygen (k_q *ca.* 1.0×10^9 M^{-1} s^{-1}). The observations support its assignment to triplet–triplet absorption. The quantum yield for intersystem crossing (Φ_{ISC}), yielding the excited triplet state, was determined as 0.51–0.63 (see Table 3).

The detection of the near-infrared luminescence of $^1O_2$ at 1276 nm (τ = 35.8 μs in toluene) provided direct evidence for the sensitization quality of **1–3**. The quantum yields of $^1O_2$ formation (Φ_Δ) were determined as being in the range of 0.50 to 0.66, constituting significant figures for heavy-atom free organoboron photosensitizers.[38,63–65] The quantum yield values of triplet formation and $^1O_2$ formation are practically the same, pointing to the fact that energy transfer from the excited triplet state of the dye to triplet oxygen proceeds with unit efficiency. It is noteworthy that the $^1O_2$ formation efficiency of the bis-borylated dye **1** is practically twice the value that was recently published by us for dye **C** (R = H; see Fig. 1).[66] This points to the importance of the higher symmetry and rigidity of dye **1**, shutting down non-radiative excited singlet-state decay other than ISC. This is in agreement with the observation that the quantum yields of fluorescence (Φ_f) and triplet state formation (Φ_{ISC}) sum up to nearly 1 for the investigated dyes (see data in Tables 1 and 3).

Being efficient photosensitizers of $^1O_2$ formation, we strived to test the photostability and resistance toward $^1O_2$-induced oxidation of the dyes in air-equilibrated toluene solution. The herein investigated dyes show degradation on prolonged irradiation (λ_{exc} > 395 nm), monitored by the decrease of the long-wavelength absorption band (see the ESI‡). However, this is most notable for **1** (46% decrease after 4 hours of irradiation) and **2** (66% decrease), featuring the linear PAHs, while dye **3** (14% decrease) is apparently more stable. The marked photoreactivity of linear acenes towards $^1O_2$ is commonly ascribed to the formation of endoperoxides by means of a [4 + 2] cycloaddition.[32,36,67–70] Analogous chemical processes are expected for the naphthalene- and anthracene-derived **1** and **2**, respectively. Similar pyrene oxidation products by the action of $^1O_2$ are not described. However, there are indications that photooxidations of this PAH ultimately lead to pyrenequinones (1,6- and 1,8-isomers).[71]

Conclusions

Bis-borylated isoquinoline-derived dyes with polycyclic aromatic cores are an interesting family of compounds with potential for bimodal activity as fluorophores and $^1O_2$ photosensitizers. They can be structurally designed as to avoid non-radiative excited singlet state deactivation other than intersystem crossing. In the best cases, 50% of the excited singlet state are channeled to fluorescence and 50% form an excited triplet state by intersystem crossing. The latter sensitizes singlet oxygen by nearly quantitative energy transfer to triplet oxygen. The thorough photophysical characterization opens perspectives for new organoboron chromophores with potential for imaging and therapeutic action. Future work will be directed towards the synthetic integration of polar groups that allow water solubility.

Conflicts of interest

There are no conflicts to declare.

Acknowledgements

We are grateful for financial support from the Spanish Ministerio de Ciencia e Innovación (grant PID2020-119992GB-I00 for U. P., PID2019-106358GB-C21 and PID2019-106358GB-C22 for A. R., PID2019-110441RB-C33 for F. B., PID2019-104293GB-I00 for F. N and E. P.-I, and doctoral fellowship PRE2020-092646 for P. V.-D.), the European Research and Development Fund (ERDF), the Consejo Superior de Investigaciones Científicas (grant 202080I005 for A. R.), the Junta de Andalucía/University of Malaga (grant UMA18-FEDERJA-007 for F. N. and E. P.-I.), and the Junta de Andalucía/University of Huelva (grant UHU-202070 for U. P.). Dr Z. Domínguez (University of Huelva) is acknowledged for technical assistance in the early phase of this work.

References

1 A. Loudet and K. Burgess, BODIPY Dyes and Their Derivatives: Syntheses and Spectroscopic Properties, *Chem. Rev.*, 2007, **107**, 4891–4932.
2 G. Ulrich, R. Ziessel and A. Harriman, The Chemistry of Fluorescent Bodipy Dyes: Versatility Unsurpassed, *Angew. Chem., Int. Ed.*, 2008, **47**, 1184–1201.
3 Z. M. Hudson and S. Wang, Impact of Donor-Acceptor Geometry and Metal Chelation on Photophysical Properties

 This journal is © the Partner Organisations 2022

Open Access Article. Published on 29 2022. Downloaded on 12/13/2025 6:14:51 PM.
This article is licensed under a Creative Commons Attribution-NonCommercial 3.0 Unported Licence.

and Applications of Triarylboranes, *Acc. Chem. Res.*, 2009, **42**, 1584–1596.

4 Y.-L. Rao and S. Wang, Four-Coordinate Organoboron Compounds with a π-Conjugated Chelate Ligand for Optoelectronic Applications, *Inorg. Chem.*, 2011, **50**, 12263–12274.

5 D. Frath, J. Massue, G. Ulrich and R. Ziessel, Luminescent Materials: Locking π-Conjugated and Heterocyclic Ligands with Boron(III), *Angew. Chem., Int. Ed.*, 2014, **53**, 2290–2310.

6 L. Ji, S. Griesbeck and T. B. Marder, Recent Developments in and Perspectives on Three-Coordinate Boron Materials: A Bright Future, *Chem. Sci.*, 2017, **8**, 846–863.

7 A. G. Bonn and O. S. Wenger, Charge Transfer Emission in Oligotriarylamine–Triarylborane Compounds, *J. Org. Chem.*, 2015, **80**, 4097–4107.

8 Z. Zhang, R. M. Edkins, J. Nitsch, K. Fucke, A. Eichhorn, A. Steffen, Y. Wang and T. B. Marder, D–π-A Triarylboron Compounds with Tunable Push–Pull Character Achieved by Modification of Both the Donor and Acceptor Moieties, *Chem. – Eur. J.*, 2015, **21**, 177–190.

9 Z. Zhang, R. M. Edkins, J. Nitsch, K. Fucke, A. Steffen, L. E. Longobardi, D. W. Stephan, C. Lambert and T. B. Marder, Optical and Electronic Properties of Air-Stable Organoboron Compounds with Strongly Electron-Accepting Bis(fluoromesityl)boryl Groups, *Chem. Sci.*, 2015, **6**, 308–321.

10 Z.-Q. Liu, Q. Fang, D. Wang, G. Xue, W.-T. Yu, Z.-S. Shao and M.-H. Jiang, Trivalent boron as acceptor in D–π-A chromophores: synthesis, structure and fluorescence following single- and two-photon excitation, *Chem. Commun.*, 2002, 2900–2901.

11 Z.-Q. Liu, Q. Fang, D. Wang, D.-X. Cao, G. Xue, W.-T. Yu and H. Lei, Trivalent Boron as an Acceptor in Donor-π-Acceptor-Type Compounds for Single- and Two-Photon Excited Fluorescence, *Chem. – Eur. J.*, 2003, **9**, 5074–5084.

12 Z.-Q. Liu, Q. Fang, D.-X. Cao, D. Wang and G.-B. Xu, Triaryl Boron-Based A-π-A vs Triaryl Nitrogen-Based D-π-D Quadrupolar Compounds for Single- and Two-Photon Excited Fluorescence, *Org. Lett.*, 2004, **6**, 2933–2936.

13 J. C. Collings, S.-Y. Poon, C. Le Droumaguet, M. Charlot, C. Katan, L.-O. Pålsson, A. Beeby, J. A. Mosely, H. M. Kaiser, D. Kaufmann, W.-Y. Wong, M. Blanchard-Desce and T. B. Marder, The Synthesis and One- and Two-Photon Optical Properties of Dipolar, Quadrupolar and Octupolar Donor–Acceptor Molecules Containing Dimesitylboryl Groups, *Chem. – Eur. J.*, 2009, **15**, 198–208.

14 S. Griesbeck, E. Michail, F. Rauch, H. Ogasawara, C. Wang, Y. Sato, R. Edkins, Z. Zhang, M. Taki, C. Lambert, S. Yamaguchi and T. B. Marder, The Effect of Branching on One- and Two-Photon Absorption, Cell Viability and Localization of Cationic Triarylborane Chromophores with Dipolar vs. Octupolar Charge Distributions for Cellular Imaging, *Chem. – Eur. J.*, 2019, **25**, 13164–13175.

15 S. Griesbeck, E. Michail, C. Wang, H. Ogasawara, S. Lorenzen, L. Gerstner, T. Zang, J. Nitsch, Y. Sato, R. Bertermann, M. Taki, C. Lambert, S. Yamaguchi and T. B. Marder, Tuning the π-Bridge of Quadrupolar Triarylborane Chromophores for One- and Two-Photon Excited Fluorescence Imaging of Lysosomes in Live Cells, *Chem. Sci.*, 2019, **10**, 5405–5422.

16 A. Wakamiya, T. Taniguchi and S. Yamaguchi, Intramolecular B–N Coordination as a Scaffold for Electron-Transporting Materials: Synthesis and Properties of Boryl-Substituted Thienylthiazoles, *Angew. Chem., Int. Ed.*, 2006, **45**, 3170–3173.

17 B. J. Liddle, R. M. Silva, T. J. Morin, F. P. Macedo, R. Shukla, S. V. Lindeman and J. R. Gardinier, BORAZANs: Tunable Fluorophores Based on 2-(Pyrazolyl)aniline Chelates of Diphenylboron, *J. Org. Chem.*, 2007, **72**, 5637–5646.

18 D. Frath, S. Azizi, G. Ulrich, P. Retailleau and R. Ziessel, Facile Synthesis of Highly Fluorescent *Borani*l, Complexes, *Org. Lett.*, 2011, **13**, 3414–3417.

19 D. Frath, A. Poirel, G. Ulrich, A. De Nicola and R. Ziessel, Fluorescent Boron(III) Iminocoumarins (Boricos), *Chem. Commun.*, 2013, **49**, 4908–4910.

20 V. F. Pais, J. M. Lassaletta, R. Fernández, H. S. El-Sheshtawy, A. Ros and U. Pischel, Organic Fluorescent Thermometers Based on Borylated Arylisoquinoline Dyes, *Chem. – Eur. J.*, 2014, **20**, 7638–7645.

21 V. F. Pais, M. M. Alcaide, R. López-Rodríguez, D. Collado, F. Nájera, E. Pérez-Inestrosa, E. Álvarez, J. M. Lassaletta, R. Fernández, A. Ros and U. Pischel, Strongly Emissive and Photostable Four-Coordinate Organoboron *N*,*C* Chelates and Their Use in Fluorescence Microscopy, *Chem. – Eur. J.*, 2015, **21**, 15369–15376.

22 S. P. J. T. Bachollet, D. Volz, B. Fiser, S. Münch, F. Rönicke, J. Carrillo, H. Adams, U. Schepers, E. Gómez-Bengoa, S. Bräse and J. P. A. Harrity, A Modular Class of Fluorescent Difluoroboranes: Synthesis, Structure, Optical Properties, Theoretical Calculations and Applications for Biological Imaging, *Chem. – Eur. J.*, 2016, **22**, 12430–12438.

23 B. Lee, B. G. Park, W. Cho, H. Y. Lee, A. Olasz, C.-H. Chen, S. B. Park and D. Lee, BOIMPY: Fluorescent Boron Complexes with Tunable and Environment-Responsive Light-Emitting Properties, *Chem. – Eur. J.*, 2016, **22**, 17321–17328.

24 V. F. Pais, P. Ramírez-Lopez, A. Romero-Arenas, D. Collado, F. Nájera, E. Pérez-Inestrosa, R. Fernández, J. M. Lassaletta, A. Ros and U. Pischel, Red-Emitting Tetracoordinate Organoboron Chelates: Synthesis, Photophysical Properties, and Fluorescence Microscopy, *J. Org. Chem.*, 2016, **81**, 9605–9611.

25 J. Wang, Q. Wu, C. Yu, Y. Wei, X. Mu, E. Hao and L. Jiao, Aromatic Ring Fused BOPHYs as Stable Red Fluorescent Dyes, *J. Org. Chem.*, 2016, **81**, 11316–11323.

26 J. H. Golden, J. W. Facendola, D. Sylvinson, M. R. C. Quintana Baez, P. I. Djurovich and M. E. Thompson, Boron Dipyridylmethene (DIPYR) Dyes: Shedding Light on Pyridine-Based Chromophores, *J. Org. Chem.*, 2017, **82**, 7215–7222.

27 Z. Domínguez, R. López-Rodríguez, E. Álvarez, S. Abbate, G. Longhi, U. Pischel and A. Ros, Azabora[5]helicene

Open Access Article. Published on 29 2022. Downloaded on 12/13/2025 6:14:51 PM. This article is licensed under a Creative Commons Attribution-NonCommercial 3.0 Unported Licence.

Charge-Transfer Dyes Show Efficient and Spectrally Variable Circularly Polarized Luminescence, *Chem. – Eur. J.*, 2018, **24**, 12660–12668.

28 Y.-L. Rao, H. Amarne, S.-B. Zhao, T. M. McCormick, S. Martić, Y. Sun, R.-Y. Wang and S. Wang, Reversible Intramolecular C-C Bond Formation/Breaking and Color Switching Mediated by a N,C-Chelate in (2-ph-py)$BMes_2$ and (5-$BMes_2$-2-ph-py)$BMes_2$, *J. Am. Chem. Soc.*, 2008, **130**, 12898–12900.

29 C. Baik, Z. M. Hudson, H. Amarne and S. Wang, Enhancing the Photochemical Stability of *N*,*C*-Chelate Boryl Compounds: C-C Bond Formation versus C=C Bond *cis*,*trans*-Isomerization, *J. Am. Chem. Soc.*, 2009, **131**, 14549–14559.

30 H. Amarne, C. Baik, S. K. Murphy and S. Wang, Steric and Electronic Influence on Photochromic Switching of *N*,*C*-Chelate Four-Coordinate Organoboron Compounds, *Chem. – Eur. J.*, 2010, **16**, 4750–4761.

31 A. C. Shaikh, D. S. Ranade, S. Thorat, A. Maity, P. P. Kulkarni, R. G. Gonnade, P. Munshi and N. T. Patil, Highly Emissive Organic Solids with Remarkably Broad Color Tunability Based on *N*,*C*-Chelate, Four-Coordinate Organoborons, *Chem. Commun.*, 2015, **51**, 16115–16118.

32 K. Liu, R. A. Lalancette and F. Jäkle, B–N Lewis Pair Functionalization of Anthracene: Structural Dynamics, Optoelectronic Properties, and O2 Sensitization, *J. Am. Chem. Soc.*, 2017, **139**, 18170–18173.

33 M. Vanga, R. A. Lalancette and F. Jäkle, Controlling the Optoelectronic Properties of Pyrene by Regioselective Lewis Base-Directed Electrophilic Aromatic Borylation, *Chem. – Eur. J.*, 2019, **25**, 10133–10140.

34 J. Full, S. P. Panchal, J. Götz, A.-M. Krause and A. Nowak-Król, Modular Synthesis of Organoboron Helically Chiral Compounds: Cutouts from Extended Helices, *Angew. Chem., Int. Ed.*, 2021, **60**, 4350–4357.

35 S. Wang, K. Yuan, M.-F. Hu, X. Wang, T. Peng, N. Wang and Q.-S. Li, Cleavage of Unstrained C-C Bonds in Acenes by Boron and Light: Transformation of Naphthalene into Benzoborepin, *Angew. Chem., Int. Ed.*, 2018, **57**, 1073–1077.

36 M. Vanga, A. Sahoo, R. A. Lalancette and F. Jäkle, Linear Extension of Anthracene via B←N Lewis Pair Formation: Effects on Optoelectronic Properties and Singlet O2 Sensitization, *Angew. Chem.*, 2022, **61**, e202113075.

37 Y. Wang, H. Chen, C. Li and P. Wu, Octachloro-fluorescein: Synthesis and photosensitizer performance evaluation, *Dyes Pigm.*, 2019, **170**, 107635.

38 R. Prieto-Montero, A. Prieto-Castañeda, R. Sola-Llano, A. R. Agarrabeitia, D. García-Fresnadillo, I. López-Arbeloa, A. Villanueva, M. J. Ortiz, S. de la Moya and V. Martínez-Martínez, Exploring BODIPY Derivatives as Singlet Oxygen Photosensitizers for PDT, *Photochem. Photobiol.*, 2020, **96**, 458–477.

39 J. Deckers, T. Cardeynaels, S. Doria, N. Tumanov, A. Lapini, A. Ethirajan, M. Ameloot, J. Wouters, M. Di Donato, B. R. Champagne and W. Maes, Balancing fluorescence and singlet oxygen formation in push-pull type near-infrared BODIPY photosensitizers, *J. Mater. Chem. C*, 2022, **10**, 9344–9355.

40 A. Kamkaew, S. H. Lim, H. B. Lee, L. V. Kiew, L. Y. Chung and K. Burgess, BODIPY dyes in photodynamic therapy, *Chem. Soc. Rev.*, 2013, **42**, 77–88.

41 K. Xu, Y. Fu, Y. Zhou, F. Hennersdorf, P. Machata, I. Vincon, J. J. Weigand, A. A. Popov, R. Berger and X. Feng, Cationic Nitrogen-Doped Helical Nanographenes, *Angew. Chem., Int. Ed.*, 2017, **56**, 15876–15881.

42 S. Liu, C. Li, Y. Xu, Z. Li, H. Huang, N. Fu, J. Shao, B. Zhao, H. Huang and W. Huang, Optoelectronic properties and aggregation effects on the performance of planar versus, contorted pyrene-cored perylenediimide dimers for organic solar cells, *Dyes Pigm.*, 2020, **173**, 107976.

43 A. Ros, B. Estepa, R. López-Rodríguez, E. Álvarez, R. Fernández and J. M. Lassaletta, Use of hemilabile *N*,*N* ligands in nitrogen-directed iridium-catalyzed borylations of arenes, *Angew. Chem., Int. Ed.*, 2011, **50**, 11724–11728.

44 J. E. Ehrlich, X. L. Wu, I.-Y. S. Lee, Z.-Y. Hu, H. Röckel, S. R. Marder and J. W. Perry, Two-photon absorption and broadband optical limiting with bis-donor stilbenes, *Opt. Lett.*, 1997, **22**, 1843–1845.

45 M. Albota, D. Beljonne, J.-L. Brédas, J. E. Ehrlich, J.-Y. Fu, A. A. Heikal, S. E. Hess, T. Kogej, M. D. Levin, S. R. Marder, D. McCord-Maughon, J. W. Perry, H. Röckel, M. Rumi, G. Subramaniam, W. W. Webb, X.-L. Wu and C. Xu, Design of Organic Molecules with Large Two-Photon Absorption Cross Sections, *Science*, 1998, **281**, 1653–1656.

46 T. Kogej, D. Beljonne, F. Meyers, J. W. Perry, S. R. Marder and J. L. Brédas, Mechanisms for enhancement of two-photon absorption in donor-acceptor conjugated chromophores, *Chem. Phys. Lett.*, 1998, **298**, 1–6.

47 B. A. Reinhardt, L. L. Brott, S. J. Clarson, A. G. Dillard, J. C. Bhatt, R. Kannan, L. Yuan, G. S. He and P. N. Prasad, Highly Active Two-Photon Dyes: Design, Synthesis, and Characterization toward Application, *Chem. Mater.*, 1998, **10**, 1863–1874.

48 S.-J. Chung, K.-S. Kim, T.-C. Lin, G. S. He, J. Swiatkiewicz and P. N. Prasad, Cooperative Enhancement of Two-Photon Absorption in Multi-branched Structures, *J. Phys. Chem. B*, 1999, **103**, 10741–10745.

49 L. Ventelon, S. Charier, L. Moreaux, J. Mertz and M. Blanchard-Desce, Nanoscale Push-Push Dihydrophenanthrene Derivatives as Novel Fluorophores for Two-Photon-Excited Fluorescence, *Angew. Chem., Int. Ed.*, 2001, **40**, 2098–2101.

50 S.-J. Chung, M. Rumi, V. Alain, S. Barlow, J. W. Perry and S. R. Marder, Strong, Low-Energy Two-Photon Absorption in Extended Amine-Terminated Cyano-Substituted Phenylenevinylene Oligomers, *J. Am. Chem. Soc.*, 2005, **127**, 10844–10845.

51 M. Pawlicki, H. A. Collins, R. G. Denning and H. L. Anderson, Two-Photon Absorption and the Design of Two-Photon Dyes, *Angew. Chem., Int. Ed.*, 2009, **48**, 3244–3266.

Open Access Article. Published on 29 2022. Downloaded on 12/13/2025 6:14:51 PM.
This article is licensed under a Creative Commons Attribution-NonCommercial 3.0 Unported Licence.

52 M. Rumi and J. W. Perry, Two-photon absorption: an overview of measurements and principles, *Adv. Opt. Photonics*, 2010, **2**, 451–518.
53 Q. Zheng, G. Xu and P. N. Prasad, Conformationally Restricted Dipyrromethene Boron Difluoride (BODIPY) Dyes: Highly Fluorescent, Multicolored Probes for Cellular Imaging, *Chem. – Eur. J.*, 2008, **14**, 5812–5819.
54 P. Didier, G. Ulrich, Y. Mély and R. Ziessel, Improved push-pull-push *E*-Bodipy fluorophores for two-photon cell-imaging, *Org. Biomol. Chem.*, 2009, **7**, 3639–3642.
55 X. Zhang, Y. Xiao, J. Qi, J. Qu, B. Kim, X. Yue and K. D. Belfield, Long-Wavelength, Photostable, Two-Photon Excitable BODIPY Fluorophores Readily Modifiable for Molecular Probes, *J. Org. Chem.*, 2013, **78**, 9153–9160.
56 M. M. Alcaide, F. M. F. Santos, V. F. Pais, J. I. Carvalho, D. Collado, E. Pérez-Inestrosa, J. F. Arteaga, F. Boscá, P. M. P. Gois and U. Pischel, Electronic and Functional Scope of Boronic Acid Derived Salicylidenehydrazone (BASHY) Complexes as Fluorescent Dyes, *J. Org. Chem.*, 2017, **82**, 7151–7158.
57 F. M. F. Santos, Z. Domínguez, J. P. L. Fernandes, C. Parente Carvalho, D. Collado, E. Pérez-Inestrosa, M. V. Pinto, A. Fernandes, J. F. Arteaga, U. Pischel and P. M. P. Gois, Cyanine-like boronic acid derived salicylidenehydrazone complexes (Cy-BASHY) for bioimaging applications, *Chem. – Eur. J.*, 2020, **26**, 14064–14069.
58 Á. Moneo Marín, J. P. Telo, D. Collado, F. Nájera, E. Pérez-Inestrosa and U. Pischel, Bis(dioxaborine) Dyes with Variable π-Bridges: Towards Two-Photon Absorbing Fluorophores with Very High Brightness, *Chem. – Eur. J.*, 2018, **24**, 2929–2935.
59 M. Tasior, P. Kowalczyk, M. Przybył, M. Czichy, P. Janasik, M. H. E. Bousquet, M. Łapkowski, M. Rammo, A. Rebane, D. Jacquemin and D. T. Gryko, Going beyond the borders: pyrrolo[3,2-b]pyrroles with deep red emission, *Chem. Sci.*, 2021, **12**, 15935–15946.
60 C. Adamo and V. Barone, Toward reliable density functional methods without adjustable parameters: The PBE0 model, *J. Chem. Phys.*, 1999, **110**, 6158–6170.
61 M. Ernzerhof and G. E. Scuseria, Assessment of the Perdew–Burke–Ernzerhof exchange-correlation functional, *J. Chem. Phys.*, 1999, **110**, 5029–5036.
62 J. Tomasi, B. Mennucci and R. Cammi, Quantum Mechanical Continuum Solvation Models, *Chem. Rev.*, 2005, **105**, 2999–3094.
63 S. Duman, Y. Cakmak, S. Kolemen, E. U. Akkaya and Y. Dede, Heavy Atom Free Singlet Oxygen Generation: Doubly Substituted Configurations Dominate S_1 States of Bis-BODIPYs, *J. Org. Chem.*, 2012, **77**, 4516–4527.
64 S. Kolemen, M. Işık, G. M. Kim, D. Kim, H. Geng, M. Buyuktemiz, T. Karatas, X.-F. Zhang, Y. Dede, J. Yoon and E. U. Akkaya, Intracellular Modulation of Excited-State Dynamics in a Chromophore Dyad: Differential Enhancement of Photocytotoxicity Targeting Cancer Cells, *Angew. Chem., Int. Ed.*, 2015, **54**, 5340–5344.
65 N. Epelde-Elezcano, E. Palao, H. Manzano, A. Prieto-Castañeda, A. R. Agarrabeitia, A. Tabero, A. Villanueva, S. de la Moya, I. López-Arbeloa, V. Martínez-Martínez and M. J. Ortiz, Rational Design of Advanced Photosensitizers Based on Orthogonal BODIPY Dimers to Finely Modulate Singlet Oxygen Generation, *Chem. – Eur. J.*, 2017, **23**, 4837–4848.
66 F. Boscá, M. C. Cuquerella, V. F. Pais, A. Ros and U. Pischel, Excited-State Pathways of Four-Coordinate *N*,*C*-Chelate Organoboron Dyes, *ChemPhotoChem*, 2018, **2**, 34–41.
67 J.-M. Aubry, C. Pierlot, J. Rigaudy and R. Schmidt, Reversible Binding of Oxygen to Aromatic Compounds, *Acc. Chem. Res.*, 2003, **36**, 668–675.
68 W. Fudickar, A. Fery and T. Linker, Reversible Light and Air-Driven Lithography by Singlet Oxygen, *J. Am. Chem. Soc.*, 2005, **127**, 9386–9387.
69 K. Liu, R. A. Lalancette and F. Jäkle, Tuning the Structure and Electronic Properties of B–N Fused Dipyridylanthracene and Implications on the Self-Sensitized Reactivity with Singlet Oxygen, *J. Am. Chem. Soc.*, 2019, **141**, 7453–7462.
70 W. Fudickar and T. Linker, Photooxygenation of Naphthalene, *ChemPhotoChem*, 2021, **5**, 1004–1008.
71 M. Sigman, P. F. Schuler, M. M. Ghosh and R. T. Dabestani, Mechanism of Pyrene Photochemical Oxidation in Aqueous and Surfactant Solutions, *Environ. Sci. Technol.*, 1998, **32**, 3980–3985.